Available online at www.sciencedirect.com
ScienceDirect
Chemical Physics Letters 443 (2007) 398–407
CHEMICAL PHYSICS LETTERS
www.elsevier.com/locate/cplett

Accurate global *ab initio* potentials at low-cost by correlation scaling and extrapolation to the one-electron basis set limit

A.J.C. Varandas *

Departamento de Química, Universidade de Coimbra 3004-535 Coimbra, Portugal

Received 16 April 2007; in final form 24 May 2007
Available online 17 June 2007

Abstract

A recently proposed scheme that enables a potential energy surface corresponding to a calculation with a large target basis set to be obtained from small basis set calculations via scaling of the electron correlation at a single-pivotal geometry is generalized to include an arbitrary number of such geometries. If the correlation is extrapolated to the complete basis set limit at the pivotal geometries and used for the scaling, the method can yield accurate potentials at costs up to factors nearly fifty times cheaper than required otherwise. The approach, free from parameters alien to the *ab initio* methods, is tested on N_2, O_2, and F_2.
© 2007 Elsevier B.V. All rights reserved.

1. Introduction

The cost of solving the electronic Schrödinger equation point-by-point to generate a potential energy surface (PES) is well known to grow as $N_p^\tau n_b^m$ with $m \gtrsim 4$, where n_b is the number of orbitals in the basis set, and N_p a typical number of points required to represent a one-dimensional (1D) cut in the τD configuration space of the molecule. Of course, many such 'diatomic-like' cuts will be required to map the PES of a polyatomic molecule, e.g., one for each fixed set of Jacobi angles. An even stronger factorial scaling of the cost with the number of active electrons (n_e) arises if the multi-reference configuration interaction (MRCI) method which is based on the preceding complete-active-space self-consistent-field (CASSCF or CAS for brevity) approach is utilized as for a fixed number of electrons the number of determinants in a full CI (the CAS wave function is a FCI in the active orbital space) scales [1] as $n_b^{n_e}$. Obtaining an accurate PES with as low as possible computational cost remains therefore an important challenge in quantum chemistry. Without any lack of generality, the 'economical' approach here suggested will be tested on the important N_2, O_2, and F_2 molecules. The highly successful internally contracted MRCI approach with the popular quasi-degenerate Davidson correction [CAS/MRCI(Q) or simply MRCI(Q)] [2,3] will be employed for the calculations.

A significant enhancement to progress in *ab initio* calculations for small molecules has become possible after the introduction of the so-called correlation-consistent (cc) basis sets by Dunning and collaborators [4] such as the augmented one aug-cc-pVXZ [5] (or AVXZ). Built in a systematic manner intended to relate the correlation energy to the cardinal number X, such basis sets prompted the search for laws to extrapolate the energy to the complete basis set (CBS) limit (e.g., Refs. [6–10]).

The extrapolation of the correlation energy finds support on its dependence on the partial wave quantum number for two-electron atomic systems and second-order pair energies in many-electron atoms [11,12]. The simplest and most popular two-parameter law for extrapolation of the correlation energy is [6]

$$E_X^{\mathrm{cor}} = E_\infty^{\mathrm{cor}} + \frac{A_3}{(X+\alpha)^3} \tag{1}$$

where E_X^{cor} is the correlation energy obtained with the X-tuple basis set of (aug)cc quality, and E_∞^{cor} and A_3 are parameters usually determined from the calculations for

* Fax: +351 239 835867.
E-mail address: varandas@qtvs1.qui.uc.pt.

0009-2614/$ - see front matter © 2007 Elsevier B.V. All rights reserved.
doi:10.1016/j.cplett.2007.06.061

the two highest affordable values of X, often 5 and 6; α is an offset parameter fixed from some auxiliary condition.

Generalized three-parameter extrapolation rules have also been suggested

$$E_X = E_\infty + \frac{A_3}{(X+\alpha)^3} + \frac{A_n}{(X+\alpha)^n} \tag{2}$$

In particular, by choosing A_n, with $n = 4$, to depend on A_3, we have suggested [8] an effective two-parameter rule that predicts the estimated CBS correlation energy limit with a root mean squared deviation (rmsd) of only a few millihartree for a set of 33 systems studied by the popular single-reference Møller–Plesset (MP2), and coupled cluster [CCSD and CCSD(T)] methods. Recently, we have shown that both the full correlation and its dynamical part can be rather accurately described via a refinement of the above law, termed as uniform singlet- and triplet-pair extrapolation (USTE [10]) method. With $n = 5$ and $\alpha = 3/8$, the auxiliary relation assumes the form [10]

$$A_5 = A_5(0) + cA_3^{5/4} \tag{3}$$

where $A_5(0) = 0.0037685459$ and $c = -1.17847713E_h^{-5/4}$ for the dynamical correlation.

For the uncorrelated Hartree–Fock and CAS (uncorrelated in the sense of lacking dynamical correlation) energies, several schemes have been advanced (Refs. [13,10], and references therein). We will use the form

$$E_X^{\mathrm{CAS}} = E_\infty^{\mathrm{CAS}} + A\exp(-bX) \tag{4}$$

where E_∞^{CAS}, A, and b are parameters to be determined from a fit to the raw CAS energies, typically the ones calculated for the three or more highest affordable cardinal numbers. Such extrapolations are known to attain a high accuracy when raw energies up to $X = 6$ are utilized, and we utilize one such variant [10]. The situation is less clear when only raw data up to $X = Q$ is available, although we will consider later also the two-point extrapolation formula proposed by Karton and Martin [13], $A + B/X^{5.34}$.

Note that the extrapolation of E_X^{CAS} and E_X^{cor} with X is geometry-dependent, and hence such a procedure for calculating a molecular PES must be carried out pointwise. This can be a mammoth task even for the fastest computers if the raw data requires basis sets with large cardinal numbers. Although the USTE [10,14] scheme has shown great promise in extrapolating from (T,Q) cardinal number pairs, we explore in this work ways for a further drastic reduction in labor by obtaining the dynamical correlation at the MRCI(Q)/AVQZ basis set level via a correlation scaling (CS) procedure recently suggested by Varandas and Piecuch [15]. This is based on scaling at a single geometry in configuration space (hereby called as pivotal geometry or simply pivot) the difference between the total energy E and the energy of some reference wave function, E^{ref}, which represents the correlation energy or part of it. In the case of the MRCI(Q) method here employed, the reference wave function is obtained in the preceding CAS calculations (see Ref. [15] for alternative choices using other quantum methods).

The approach here suggested involves six steps: (a) calculation of the PES at, say N_{p} points, with the $X-2$ and $X-1$ basis sets using MRCI(Q), and $N = 1$–4 such calculations with the target basis set of rank X at some pre-chosen pivots (see later); (b) $N_{\mathrm{p}} - N$ calculations of the CAS (here taken as the reference) PES at the target X basis set level; (c) prediction by extrapolation [10,13] to $X = \infty$ of the CAS/CBS PES; (d) prediction by extrapolation to $X = \infty$ of the dynamical correlation energy at the pivots by using the USTE/(T,Q) method [10]; (e) prediction of the CBS dynamical correlation at the remaining $N_{\mathrm{p}} - N$ points by CS using the $X = T$ (or $X = D$) and the CBS dynamical correlation energies at the N pivots; (f) calculation of the full CBS PES by adding the CAS/CBS and extrapolated dynamical correlation energies from steps (c) and (d,e). For brevity such CAS/CBS + CS^N/USTE energies will be denoted heretofore without apparent confusion by CS^N/USTE. For specificity, we indicate after the acronym USTE the cardinal number pair associated to the raw dynamical correlation energies utilized for the extrapolation.

In the following, we will consider AVQZ as an expensive basis set, as it is perhaps the largest affordable basis for small molecules. Thus, except for the MRCI(Q)/AVQZ calculations at $N = 1$–4 pivotal geometries, the bulk calculations employ only the modest AVDZ and AVTZ basis sets. The quality of the CS^N/USTE(T,Q) potentials so obtained will then be tested through vibrational calculations, which provide a most severe test of the method as the results depend on relative energies. The Letter is organized as follows. In Section 2, we describe the correlation scaling-extrapolation procedure to obtain the PES at the target basis set, while the results are reported and discussed in Section 3. The concluding remarks are in Section 4.

2. Generalized correlation scaling-extrapolation method

Let without any lack of generality from the computational point of view consider a PES as a bunch of 1D cuts through its configuration space. Let the appropriate coordinate (radial or angular or any suitable combination of both) defining the one-dimensional domain along such a cut be denoted as R. Suppose now that MRCI(Q) or some other correlated calculations using basis sets indexed by $m-k$ and m are performed ($m \equiv X$ for AVXZ, but it can be an arbitrary index for basis sets that do not belong to the cc family [15]) within such a domain. The extrapolated MRCI(Q) for the target $(m+\ell)$th basis set will be obtained from

$$E_{m+\ell}(R) = E_{m+\ell}^{\mathrm{ref}}(R) + [1 + \mathscr{P}_{m+\ell,m}^{(N)}(R)]\Delta E_m^{\mathrm{cor}}(R) \tag{5}$$

where a first choice for $\mathscr{P}_{m+\ell,m}^{(N)}(R)$ would be an interpolating polynomial of degree $N-1$ through N points $\{y_i = y(R_i)\}$ as given by the Lagrange classical formula

$$\mathscr{P}^{(N)}_{m+\ell,m}(R) = \frac{(R-R_2)(R-R_3)\cdots(R-R_N)}{(R_1-R_2)(R_1-R_3)\cdots(R_1-R_N)}y_1 + \frac{(R-R_1)(R-R_3)\cdots(R-R_N)}{(R_2-R_1)(R_2-R_3)\cdots(R_2-R_{N-1})}y_2 + \cdots + \frac{(R-R_1)(R-R_2)\cdots(R-R_{N-1})}{(R_N-R_1)(R_N-R_2)\cdots(R_N-R_{N-1})}y_N \quad (6)$$

In turn, the unitless points to be interpolated are defined by

$$y(R) = \frac{[S(R)_{m,m-k}-1][S(R_i)_{m+\ell,m}-1]}{S(R_i)_{m,m-k}-1} \quad (7)$$

where the index i specifies a pivotal geometry where the scaling is performed, k and ℓ are suitable positive integers, and the auxiliary function $S(R)$ assumes the form

$$S(R)_{m,m-k} = \Delta E^{\rm cor}_m(R)/\Delta E^{\rm cor}_{m-k}(R) \quad (8)$$

with $E^{\rm ref}_{m-k}(R)$ being the energy of the reference wave function (here taken as the CAS wave function) for the $m-k$ basis set, and $\Delta E^{\rm cor}_{m-k}(R) = E_{m-k}(R) - E^{\rm ref}_{m-k}(R)$ the associated dynamical correlation energy. Corresponding definitions apply to $\Delta E^{\rm cor}_m(R)$ and $E^{\rm ref}_{m+\ell}(R)$ in the above equations, with the latter being the energy of the reference wave function calculated with the $(m+\ell)$th target basis set. Thus, if there are N energies calculated with the $(m+\ell)$th basis set, there will be N terms in Eq. (6), each a polynomial of degree $(N-1)$ and each constructed to be zero at all R_i values but one where it is here constructed to be $y_i = y(R_i)$. In fact, Eq. (5) is perhaps the simplest mathematical expression that one can suggest to interpolate the energies based on scaling the correlation energy (or part of it if other wave function model is employed) from basis set m to basis set $m+\ell$ at the pivots. In particular, the scaling function $[1+\mathscr{P}^{(N)}_{m+\ell,m}(R)]$ in Eq. (5) satisfies the following attributes: (i) $[1+\mathscr{P}^{(N)}_{m+\ell,m}(R)] \to 1$ for all values of R when $m \to \infty$ as $y(R) \to 0$ due to $S(R)_{m,m-k} \to 1$ and $S(R)_{m+\ell,m} \to 1$, and the fact that the numerator of Eq. (7) vanishes faster than the denominator; (ii) the value of $[1+\mathscr{P}^{(N)}_{m+\ell,m}(R)]$ at any of the pivots equals the ratio of $\Delta E^{\rm cor}_{m+\ell}$ and $\Delta E^{\rm cor}_m$. If $N=1$, the method corresponds to the scheme proposed elsewhere [15]. In this case, there is a single pivot which can be the equilibrium geometry R_e or any other point on the PES. Thus, the MRCI(Q) or some other PES $E_{m+\ell}(R)$ is extrapolated from the PESs $E_m(R)$ and $E_{m-k}(R)$, the corresponding reference energies $E^{\rm ref}_{m+\ell}(R)$,$E^{\rm ref}_m(R)$ and $E^{\rm ref}_{m-k}(R)$, and N correlated energies calculated at the selected pivots (reference geometries) $R_1, R_2, \ldots, R_N$, namely $E_{m+\ell}(R_1), E_{m+\ell}(R_2), \ldots, E_{m+\ell}(R_N)$.

Although mathematically rigorous, the Lagrange formalism may yield artifacts outside the range of interpolated data, particularly when high-order polynomials are used in the interpolation procedure. We have therefore tested also a procedure based on switching forms. Although tanh functions are most popular for this purpose, we employ more flexible forms that warrant continuity up to a prechosen order $\tilde{m}-1$ in the derivatives, where $\tilde{m}$ is a positive number greater than 1, here taken as 2. For the two-pivot case (partition of the R-domain for $R \leqslant R_{\rm out}$ in two sectors: one characterizing regions up to the first pivot, $R_{\rm ref}$, the other characterizing the outer part, $R > R_{\rm ref}$), one may write:

$$y(R) = y_{\rm ref} + \Delta y_{\rm out}\{1-\exp[-\beta(R-R_{\rm ref})^{\tilde{m}}]\} \quad R \geqslant R_{\rm ref} \quad (9)$$

$$y(R) = y_{\rm ref} \quad R < R_{\rm ref} \quad (10)$$

where $\Delta y_{\rm out} = y_{\rm out} - y_{\rm ref}$, and β is chosen such that $y(R_{\rm out}) \sim y_{\rm out}$ within an acceptable tolerance (typically 0.1%). For example, a typical value of β for N_2 is 1.5 Å^{-1}, although other values close to it could work equally well or perhaps slightly better. Note that $y_{\rm out}$ is the value obtained from Eq. (7) at the pivot $R_{\rm out}$, with corresponding definitions applying for the other y_i values. Note further that $R_{\rm ref}$ has been taken as the experimental equilibrium geometry, and $R_{\rm out}$ as a geometry sufficiently far from equilibrium to represent the limiting behavior. Thus, for a diatomic, the above switching function can impose a scaling trend such as to warrant reproduction of the correct energy at the dissociation asymptote. For the three-sector case where there are an inner ($R_{\rm inn}$), an intermediate ($R_{\rm ref}$), and an outer ($R_{\rm out}$) pivots, we may write:

$$y(R) = y_{\rm inn} \quad R \leqslant R_{\rm inn} \quad (11)$$

$$y(R) = y_{\rm ref} + \Delta y_{\rm inn}\{1-\exp[-\beta_{\rm inn}(R-R_{\rm ref})^{\tilde{m}}]\} \quad R_{\rm inn} \leqslant R \leqslant R_{\rm ref} \quad (12)$$

$$y(R) = y_{\rm ref} + \Delta y_{\rm out}\{1-\exp[-\beta_{\rm out}(R-R_{\rm ref})^{\tilde{m}}]\} \quad R > R_{\rm ref} \quad (13)$$

where $\Delta y_{\rm inn} = y_{\rm inn} - y_{\rm ref}$, $\Delta y_{\rm out} = y_{\rm out} - y_{\rm ref}$, and $\beta_{\rm inn}$ and $\beta_{\rm out}$ are parameters chosen as above to satisfy the boundary conditions. For example, for N_2, typical β values are $\beta_{\rm inn} = 55.0$ Å^{-1} and $\beta_{\rm out} = 1.5$ Å^{-1}. Of course, if the innermost and outermost pivots ($y_{\rm inn}$ and $y_{\rm out}$) correspond to the extreme calculated points along the R-coordinate, only Eqs. (12) and (13) apply. Forms with more pivots can similarly be developed.

The ability of the CS method to predict the PES corresponding to larger basis sets from smaller basis set calculations with sub-millihartree accuracies suggests that the procedure can be combined with available schemes to extrapolate the PES to the CBS limit. Two distinct approaches can be followed. The first consists of treating the extrapolated USTE(T,Q) energies at the pivots as $E_{m+\ell}(R_i)$ ($i = 1-N$), and apply the above CS method. Alternatively, one could extrapolate at every point to $X = \infty$ using the raw AVTZ energies and the AVQZ ones estimated via the USTE(T,Q) scheme (or else the raw MRCI(Q)/AVQZ energies at the pivots). Since the fit of a $\tilde{n}$-parameter law to $\tilde{n}$-points is an ill-posed problem in the sense that in no way the procedure can be tested (i.e., relies on the exactness of both the numerical data and underlying physical law), we will adopt here the first scheme. If the other had been chosen, it might be advisable to employ instead the USTE($D-Q$) extrapolation scheme

[10] as this is expected to be stabilized by the use of three fitted points. The method is 'analytic' to the order imposed by the power $\tilde{m}$ in Eqs. (9)–(13) at one pivot, here chosen as $R_{\rm ref}$, and up to the allowed matching tolerance at the other pivots. Although this can be controlled such that the boundary conditions are matched to a desired accuracy, one may wish to avoid extreme cases since they originate abrupt changes in $y(R)$. Indeed, any small discontinuities in $y(R)$ and its derivatives should not be troublesome as the raw *ab initio* energies and therefore their derivatives exhibit also some inescapable numerical noise. Thus, we may for all purposes consider as smooth the resulting PES, being probably adequate for direct dynamics studies. In fact, any such small errors will likely pass unnoticed if the derivatives are calculated numerically as often done in dynamics. Finally, we emphasize that both the single-pivot and multi-pivot methods (if based on the Lagrange formalism) are analytic, with the latter showing in principle no handicap if extrapolations in R will not occur. In fact, hybrid approaches using both the Lagrange and switching-function formalisms may also be envisaged. We further note that the method has no empirically adjustable parameters, and hence contrasts with other single-pivot schemes [16–18] that extrapolate the correlation energy but choose the scaling to fit some well known experimental attribute of the molecule such as available atomization or dissociation energies.

3. Results and discussion

All MRCI(Q)/AVXZ ($X = D, T, Q$) calculations have been performed using MOLPRO [19]. As test systems, we have chosen N_2, O_2, and F_2 in their ground electronic states, as these molecules are representative of three of the most frequent types of chemical bonds (single in F_2, double in O_2, and triple in N_2). For all species, the active space in the CAS and subsequent MRCI(Q) calculations consisted of the valence orbitals that correlate with the 2s and 2p atomic shells. The lowest-energy molecular orbitals (involving the 1s orbitals) have been optimized in the CAS calculations, but their occupancies remained doubly occupied in all reference determinants that define the CAS and MRCI wave functions. For comparison purposes, MRCI(Q) calculations have also been carried out over the same range of geometries using the AV5Z and AV6Z basis sets. Although core electrons may bring significant contributions, core and core-valence correlation effects will therefore be ignored, in addition to relativistic and non-adiabatic correction effects. As indicated by the symbols in Fig. 1, the calculations covered $N_{\rm p} = 29$ geometries over the range of reduced bond distances $0.7 \leqslant R/R_{\rm e} \leqslant 5.0$, with $R_{\rm e}$ taken as the experimental equilibrium geometry [20].

Fig. 1 shows the results obtained from both the $(m,m-k;m+\ell,m) = (3,2;4,2)$ and $(3,2;4,3)$ CS schemes. The top panels illustrate the changes $\Delta E^{\rm cor}_{m+\ell,m-k} = E^{\rm cor}_{m+\ell} - E^{\rm cor}_{m-k}$ in correlation energy when going from the smaller to the target basis set, namely $\Delta E^{\rm cor}_{42} = E^{\rm cor}_4 - E^{\rm cor}_2$ and $\Delta E^{\rm cor}_{43} = E^{\rm cor}_4 - E^{\rm cor}_3$, while the corresponding errors $\epsilon^{\rm cor}_{m+\ell,m-k}$ are plotted in the bottom panels. As Fig. 1 shows, the target correlation energy is recovered within a millihartree or so accuracy when utilizing a single pivot at $R = R_{\rm e}$, but this result can be improved by a factor of at least five-fold if additional pivots are utilized. Of course, using more than four pivots would hardly fit the goal of low-cost PESs,

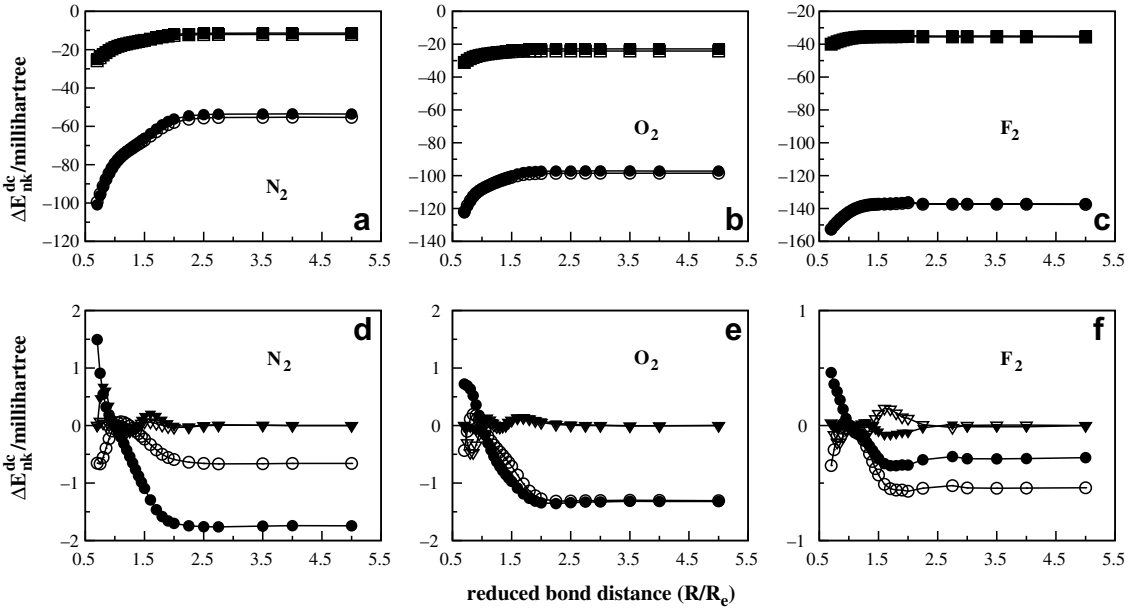

Fig. 1. A comparison of the actual and predicted changes in MRCI(Q)/AVXZ correlation energies when going from basis set $m-k$ to basis set $m+\ell$, $\Delta E_{m+\ell,m-k} = E_{m+\ell} - E_{m-k}$: (a) N_2; (b) O_2; (c) F_2. The corresponding errors when using 1 and 4 pivots are shown in panels (d)–(f). With $m = 3$ and $\ell = 1$, the dashed lines are for $k = 1$ and the solid ones for $k = 0$. The line segments that link the calculated points are drawn to guide the eye, with the points at $R/R_{\rm e} = 3$ for N_2 and $R/R_{\rm e} = 2.5$ for F_2 removed for clarity as they would originate meaningless spikes.

and hence it has not been considered. The results are best appreciated from Table 1 where the rmsd between the predicted and raw energies calculated at the target basis set level are collected. For example, in the case of N_2 at the (3,2;4,2) CS level, the rmsd varies from 0.438 (0.438) for a single pivot [15] to 0.358 (0.243), 0.259 (0.097), and 0.132 (0.100) mE_h for scaling at two, three, and four pivots using the Lagrange (switching function) formalism. Clearly, the results depend on the location of the pivots, which could be optimized to reduce the rmsd. Since this may be considered to be expensive, as there is no obvious way of finding the optimum location prior to detailed *ab initio* calculations, we have excluded such a step for generality, except in what concerns the obvious equilibrium and (the chosen) dissociation geometries. Thus, the pivots have in all cases been fixed at: R_e for the single-pivot (CS^1) case; R_e and 5 R_e for CS^2; 0.7 R_e, R_e, and 5 R_e for CS^3; 0.7 R_e, R_e, 1.4 R_e, and 5 R_e for CS^4. Our choice corresponds in CS^2 to divide the space into two sectors (up to equilibrium and beyond it, up to the chosen asymptote). For CS^3, an additional pivot has been considered at the repulsive wing of the potential (here taken as the shortest calculated bond distance), while in CS^4 the outer branch has been subdivided in two parts with the fourth pivot (point #15) being chosen as the middle point of the 29 that were calculated.

The dependence of the rmsd on the pivotal geometries may explain its non-monotonic decrease with their number. For example, for the (4,2;4,3) scheme using the Lagrange (switching) interpolation procedure, the rmsd for N_2 are 1.196 (1.196), 0.262 (0.446), 0.198 (0.341), and 0.253 (0.235) mE_h. Since the predictions for distances shorter than the first pivot and larger than the last can be erratic in the Lagrange approach, only the switching function results will be examined. Note that CS^2 suffices to mimic the diatomic atomization energy at the target basis set level. We further observe that slightly smaller errors are generally obtained when the Davidson correction is not included.

Extrapolation to the CBS limit can now be considered by using the extrapolated USTE(T,Q) correlation energies at the pivots as the results at the target $X=\infty$ basis set. For brevity, we consider only the (4,3;USTE,4) correlation scaling scheme, where USTE stands now for USTE(T,Q). Note that the error due to the USTE(T,Q) extrapolation scheme has been shown elsewhere [10] to be rather small when judged from the USTE(5,6) results. At equilibrium, they amount to [10] −0.737, −0.572, and −0.155 mE_h for N_2, O_2, and F_2, with similarly good results extending up to dissociation. Once the extrapolated (4,3;USTE,4) dynamical correlation energies have been predicted, the full extrapolated curve can be obtained by adding the reference CAS/CBS energy as predicted by our own rule [10]. This consists of extrapolating the raw CAS energies obtained with the four largest affordable AVXZ basis sets ($X=T,Q,5,6$) with the three-parameter exponential law in Eq. (4), and take as the recommended result the average of the value so obtained with the largest affordable raw

Table 1
Rmsd in up to four-pivot correlation scaling results relative to the raw MRCI(Q) dynamical-correlation energy differences

System[e,f]	$\min\Delta_{m+\ell,m-k}$ [f,g]	$\max\Delta_{m+\ell,m-k}$ [g,h]	CS^1/USTE(T,Q)[a]		CS^2/USTE(T,Q)[b]			CS^3/USTE(T,Q)[c]			CS^4/USTE(T,Q)[d]		
			$\epsilon_4^{L,s}$ [i]	%[j]	ϵ_4^{L}	%	ϵ_4^{s}	%	ϵ_4^{L}	%	ϵ_4^{s}	%	ϵ_4^{L}	%	ϵ_4^{s}	%
N_2	−100.939	−53.521	1.196	2.13	0.262	0.44	0.446	0.57	0.198	0.29	0.341	0.49	0.253	0.45	0.235	0.27
	−25.112	−11.380	0.438	3.48	0.358	1.72	0.243	1.06	0.259	2.08	0.097	0.30	0.132	0.77	0.100	0.33
O_2	−122.697	−97.171	0.957	1.04	0.309	0.33	0.292	0.28	0.189	0.20	0.150	0.16	0.069	0.07	0.074	0.08
	−30.658	−22.840	0.841	3.87	0.263	1.07	0.122	0.47	0.501	2.26	0.168	0.65	0.105	0.42	0.162	0.62
F_2	−153.004	−137.072	0.255	0.19	0.142	0.11	0.145	0.11	0.080	0.06	0.062	0.05	0.054	0.04	0.050	0.04
	−39.682	−35.020	0.379	1.15	0.169	0.49	0.090	0.25	0.317	0.97	0.064	0.19	0.085	0.26	0.079	0.24

[a] Scaling carried at pivot #7 for $R=R_e$.
[b] As in (a) but with two pivots (#7 and #29) at $R=R_e$ and $5R_e$.
[c] As in (*a*) but with three pivots (#1, #7, and #29) at $R=0.7R_e$, R_e, and $5R_e$.
[d] As in (*a*) but with four pivots (#1, #7, #15, and #29) at $R=0.7R_e$, R_e, $1.5R_e$, and R_e.
[e] For each system, the first entry refers to the (3,2;4,2) scaling (i.e., $m=3$, $k=1$, and $\ell=1$), while the second one is for (3,2;4,3) (i.e., $m=3$, $k=0$, and $\ell=1$).
[f] Largest unsigned value over the range of fitted correlation energy differences.
[g] In millihartree.
[h] Smallest unsigned value over the range of fitted correlation energy differences.
[i] The superscript 'L' refers to the Lagrange interpolation procedure, while 's' stands for switching function formalism; see the text.
[j] Indicated under the heading % at the right-hand-side of the error in millihartree is the corresponding percent error.

CAS energy ($X = 6$). Thus, we expect the CS^N/USTE(T, Q) potentials to be rather accurate, with an accuracy most likely superior to the raw AV6Z energies. They are shown in Figs. 2–4 for the ground electronic states of N_2, O_2, and F_2, with the calculated points (not shown) connected for clarity by cubic splines.

Also shown for N_2 in Fig. 2 are the extrapolated CAS and raw MRCI(Q) correlation energies, as well as the turning points [21] obtained from the RKR inversion of spectroscopic data. The notable feature is the good agreement between the extrapolated curve and the empirical RKR points. Another visible trend from the insert of this figure is the more abrupt approach to dissociation with increasing cardinal number. This may be rationalized from the well known basis set superposition error (BSSE), which tends to make the potential more attractive for poor basis sets but vanishes for an infinite basis set. The shape of the potential manifests on the calculated vibrational term values that are collected in Table 2. To reduce at a minimum any influence of fitting the calculated data to an analytic function, all ro-vibrational calculations here reported have been carried out on spline-fitted curves, suitably extrapolated to the asymptotes as implemented in Ref. [22]. Although the number of calculated raw energies may be too small for accurate spectroscopic calculations, it should suffice to warrant the trends here reported. As seen from Table 2, all CS^N/USTE(T, Q) potentials reach AV7Z or even higher quality. Although basically equivalent when judged from their rmsd, it is interesting to note that CS^1/USTE(T, Q) yields typically as accurate results as the more elaborate $CS^{N\geqslant 2}$/USTE(T, Q) ones. This may not be surprising since limited CI methods such as MRCI(Q) are well known to suffer from size-extensivity errors [23], and hence such deficiencies may extend to the CS^N/USTE(T, Q) energies. We emphasize though that only MRCI(Q) calculations using the modest AVDZ and AVTZ basis sets, and 1 to 4 points using AVQZ, have been performed.

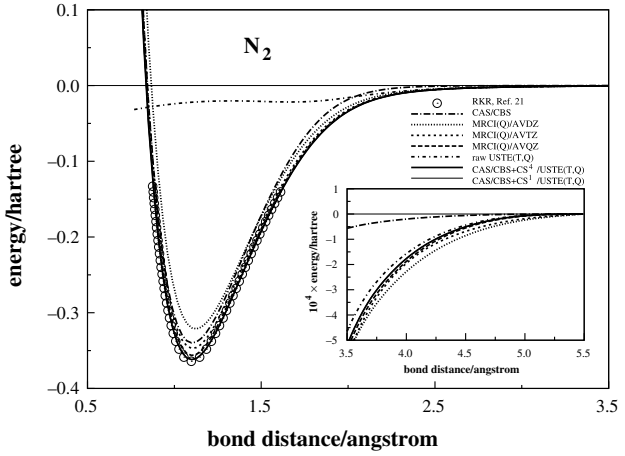

Fig. 2. Potential energy curves of N_2. Shown are the MRCI(Q)/AVXZ and CS^N/USTE(T, Q) ($N = 1,4$) curves, in addition to the USTE(T, Q) dynamical correlation, CAS/CBS, and spectroscopic RKR energies. In this and subsequent plots, the CAS/CBS energy used to calculate the CAS^N/USTE(T, Q) potentials has been obtained by using our own rule [10] with ($T, Q, 5, 6$) raw energies; see also text.

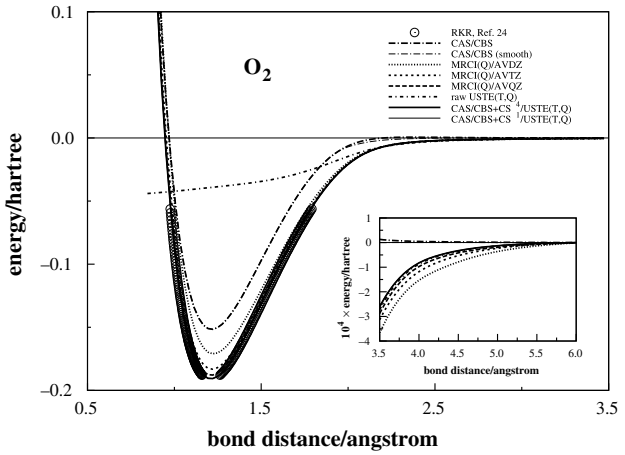

Fig. 3. As in Fig. 2 but for the ground electronic state of O_2.

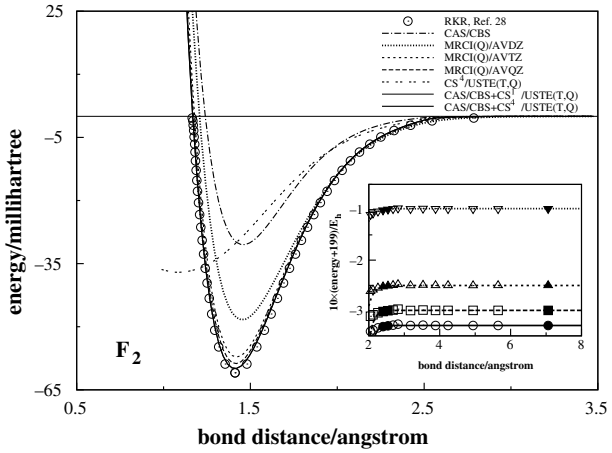

Fig. 4. As in Fig. 2, the main panel shows the potential energy curves of F_2. Shown in the insert are the 'non-smoothed' *ab initio* energies (symbols), and the corresponding 'smoothed' curves (lines; see the text) which were fitted by reproducing the (three) solid symbols. These curves are valid only after the innermost fitted point, and should illustrate the 'roughness' (as manifested by the ups and downs relative to the dissociation asymptote) of the raw *ab initio* points at intermediate bond distances, although attenuated in the scale of the figure.

The potential curves for the ground electronic state of molecular oxygen are depicted in Fig. 3. Besides some trends that are akin to N_2, the striking feature is perhaps the occurrence of a small barrier in the CAS/CBS curve (this result is common to all raw CAS/AVXZ curves), a fact that is also very much present in the case of F_2 to be discussed later. Since this barrier is small and does not show up in the MRCI(Q)/AVXZ curves, we have ignored it at first. The calculated vibrational term values are gathered in Table 2. Interestingly, the CS^1/USTE(T, Q) potential gives results as good as $CS^{N\geqslant 2}$/USTE(T, Q) when judged from the RKR turning points [24]. Somewhat surprisingly, we observe only a very small improvement when going from the raw AV5Z to AV6Z terms values. Although this might lead to conclude that the results were converged

Table 2
Vibrational term values G_v of N_2, O_2, and F_2

System	v	Theoretical[a]									exp.[f]
		AV*DZ*	AV*TZ*	AV*QZ*	AV5Z	AV6Z	CS[1 b]	CS[2 c]	CS[3 d]	CS[4 e]	
N_2	0	29.6	17.1	9.4	6.8	6.0	4.4	4.8	4.2	4.1	1175.8
	1	89.0	51.3	27.9	20.1	17.7	12.7	13.9	12.4	12.2	3505.7
	2	149.3	85.4	46.3	33.3	29.3	20.9	22.9	20.7	20.4	5806.9
	3	210.7	119.7	64.6	46.6	40.9	29.1	31.8	29.1	28.7	8079.5
	4	273.1	154.1	82.8	59.7	52.2	37.1	40.5	37.4	36.9	10323.3
	5	336.5	188.7	100.9	72.8	63.5	45.0	49.1	45.6	45.0	12538.3
	10	673.3	365.5	190.8	137.1	117.8	82.8	89.5	85.0	84.0	23180.2
	15	1051.6	551.7	280.3	199.6	169.1	117.5	125.6	120.8	119.6	33094.4
	rmsd[g]	1032.5	526.5	263.3	186.0	156.5	107.7	114.7	110.7	109.7	
							102.6	109.6	105.5	104.5	
O_2	0	22.4	15.0	4.1	2.2	2.2	0.0	−0.1	−0.4	−0.3	787.4
	1	68.6	44.5	12.0	6.1	6.0	−0.7	−1.0	−1.7	−1.3	2343.8
	2	117.1	73.3	19.7	9.7	9.6	−1.7	−2.3	−3.2	−2.5	3876.6
	3	167.5	101.4	27.3	13.0	12.9	−2.9	−3.8	−4.9	−4.0	5386.0
	4	219.8	128.9	34.6	16.1	16.0	−4.3	−5.6	−6.9	−5.6	6872.3
	5	273.8	155.7	41.8	19.0	18.9	−6.1	−7.6	−9.1	−7.4	8335.6
	10	564.3	280.0	75.7	30.7	30.2	−17.9	−21.1	−22.9	−19.4	15310.9
	15	882.6	390.8	107.4	39.0	35.5	−36.0	−40.9	−42.7	−37.5	21718.2
	rmsd[g]	772.3	332.4	91.2	32.1	29.1	34.0	38.0	39.4	35.1	
							51.1	55.2	56.7	52.3	
F_2	0	53.8	8.3	5.8	3.0	2.1	1.2	1.0	0.9	0.9	458.3
	1	156.3	20.5	12.1	3.9	1.0	−1.6	−2.2	−2.5	−2.4	1352.2
	2	259.9	34.6	19.3	5.7	0.9	−3.5	−4.5	−5.0	−4.7	2222.5
	3	364.7	50.4	27.4	8.6	1.8	−4.5	−6.1	−6.7	−6.2	3068.5
	4	470.8	68.2	36.6	12.7	4.0	−4.4	−6.6	−7.3	−6.6	3889.8
	5	578.5	88.2	47.1	18.3	7.6	−3.0	−5.9	−6.6	−5.7	4685.8
	10	1138.1	219.4	119.6	67.6	47.1	22.5	15.6	14.9	17.1	8256.8
	15	1729.2	410.3	231.7	157.1	126.4	81.7	70.2	69.6	72.6	11057.9
	rmsd[g]	1428.0	374.1	206.7	134.3	109.8	71.5	62.6	62.3	64.4	
							86.3	72.9	72.5	78.2	

[a] Deviations, $G_v^{\mathrm{exp}} - G_v^{\mathrm{calc}}$. Under the headings AV*XZ* are the results obtained for the raw MRCI(Q)/AV*XZ* calculations.
[b] Based on the CS[1]/USTE(3,4) method from the present work.
[c] As in (a) but for CS[2]/USTE(T,Q).
[d] As in (a) but for CS[3]/USTE(T,Q).
[e] As in (a) but for CS[4]/USTE(T,Q).
[f] The zero-point energy has been taken from Huber and Herzberg [20], and added to the $G(v)$ values reported in Refs. [21,24] for N_2, and O_2, respectively. See Ref. [28] for F_2.
[g] Rmsd with respect to the experimental term values: $v \leqslant 24$ for N_2; $v \leqslant 22$ for O_2; $v \leqslant 22$ for F_2. The first entry refers to the actual tabulated results, which employed CAS energies extrapolated from our own rule [10], i.e., using up to $X = 6$ raw energies, while the (T,Q) two-parameter rule of Karton and Martin [13] has been utilized for the second entry; see the text.

to within a few cm^{-1} at $X = 6$, this is clearly not the case when judging from the empirical RKR data. Besides, we should have in mind that only the first 23 vibrational levels have been counted for the statistics. We recall that a direct least-squares fit [25] to 90 ro-vibrational spectroscopic term values [26] and the 23 RKR points reported by Krupenie [24], let to an O_2 potential that reproduces the input data with a rmsd of $0.6\ \mathrm{cm}^{-1}$ for the 90 ro-vibrational energies ($1.4\ \mathrm{cm}^{-1}$ with respect to the 18 vibrational energies), and $22\ \mathrm{cm}^{-1}$ for the RKR points. Somewhat coincidentally, perhaps, we obtain a rmsd of similar order of magnitude from our CS^N/USTE(T,Q) curves. Table 3 gathers the rotational constants of O_2 for vibrational states up to $v = 21$. Despite typical deviations with respect to experiment of only $0.005\ \mathrm{cm}^{-1}$ (they are typically smaller by $10^{-3}\ \mathrm{cm}^{-1}$ for the potentials based on the CAS/CBS energies from the two-parameter (T,Q) rule of Karton and Martin [13]; see later), the results obtained from all CS^N/USTE(T,Q) potentials are better than the raw MRCI(Q)/AV5Z and AV6Z ones. A final remark to note that removing the barrier in the CAS/CBS curve (thin dash-dot line in Fig. 3) has no noticeable effect in the vibrational energies.

The calculated curves for molecular fluorine are plotted in Fig. 4. As shown in the insert of this figure, all CAS and MRCI(Q)/AV*XZ* ($X = D,T,Q,5,6$) calculations show instabilities beyond a reduced bond distance of about $R/R_e = 2.5$, i.e., $R = 3.53$ Å. In an attempt to investigate whether this could be due to the step size used for the calculations, we have performed a dense grid calculation using the AV*DZ* basis set. No changes have been observed. We have also carried out two-state averaged CAS/AV*DZ* calculations in an attempt to explore whether such instabilities could be assigned to a nearby perturbing state of the same symmetry. At this level of theory, the first excited state

Table 3
Rotational constants for the various vibrational states of O_2 in cm $^{-1}$

v	Theoretical[a]							Experimental							
	AV*DZ*	AV*TZ*	AV*QZ*	AV5Z	AV6Z	CS[1]	CS[4]	Ref. [26]	Ref. [29]	Ref. [30]	Ref. [31]	Ref. [32]	Ref. [33]	Ref. [34]	Ref. [35]
0	1.3972	1.4153	1.4273	1.4298	1.4298	1.4326	1.4326	1.4377		1.4377				1.4378	
1	1.3805	1.3996	1.4116	1.4142	1.4142	1.4170	1.4169	1.4218		1.4219				1.4220	
2	1.3639	1.3840	1.3960	1.3986	1.3986	1.4014	1.4013	1.4060		1.4061			1.4068		
3	1.3474	1.3685	1.3805	1.3831	1.3831	1.3859	1.3858	1.3904		1.3904			1.3886		
4	1.3311	1.3530	1.3650	1.3676	1.3676	1.3704	1.3703	1.3747		1.3747		1.3736	1.3742		
5	1.3148	1.3377	1.3495	1.3522	1.3522	1.3550	1.3549					1.3583	1.3590		
6	1.2985	1.3224	1.3341	1.3369	1.3369	1.3396	1.3396					1.3427			
7	1.2824	1.3071	1.3188	1.3215	1.3215	1.3243	1.3242					1.3262			
8	1.2663	1.2919	1.3035	1.3063	1.3062	1.3090	1.3089								
9	1.2502	1.2767	1.2882	1.2910	1.2909	1.2937	1.2936				1.2978				
10	1.2342	1.2614	1.2729	1.2758	1.2756	1.2784	1.2784				1.2823				
11	1.2181	1.2462	1.2576	1.2605	1.2603	1.2631	1.2631				1.2659				1.26
12	1.2020	1.2309	1.2424	1.2453	1.2450	1.2478	1.2477		1.2506						1.250
13	1.1859	1.2155	1.2271	1.2301	1.2296	1.2324	1.2323		1.2351						1.235
14	1.1696	1.2001	1.2117	1.2148	1.2141	1.2170	1.2169		1.2193						1.221
15	1.1532	1.1845	1.1962	1.1993	1.1985	1.2014	1.2013		1.2034						1.202
16	1.1367	1.1688	1.1806	1.1837	1.1829	1.1858	1.1857		1.1877						1.186
17	1.1199	1.1529	1.1648	1.1679	1.1670	1.1700	1.1699		1.1717						1.171
18	1.1029	1.1367	1.1487	1.1518	1.1510	1.1540	1.1539		1.1557						1.156
19	1.0856	1.1203	1.1322	1.1354	1.1348	1.1378	1.1377								1.139
20	1.0678	1.1036	1.1155	1.1187	1.1183	1.1213	1.1213								1.121
21	1.0495	1.0865	1.0984	1.1017	1.1014	1.1046	1.1045								1.104

[a] Notation as in Table 2.

appears well enough separated, and hence can hardly be responsible for such a disturbance. Moreover, the lower adiabatic curve continued to reveal a similar pattern, with a small bump appearing at moderate bond distances. To overcome the difficulty (which, as a matter of fact, can hardly be remedied in direct dynamics calculations using a one-state calculation), we have first attempted to fit both the raw MRCI(Q) and CS^N/USTE(T,Q) curves using the dispersion-type form $V(R) = a + b/R^6 + c/R^8$, where a is fixed at the corresponding asymptotic energy (taken as $R \sim 7$ Å), and b and c are parameters determined by, say, reproducing the two far most geometries prior to the disruption of the potential curve ($R = 2.40$ and 2.54 Å). Unfortunately, no solution free from artifacts (this would basically require both b and c to be negative such as to avoid developing a maximum before dissociation; a itself is also negative when one considers the total electronic energy) could be found. We then turned to the exponential form $V(R) = a + b\exp(cR)$, with the parameters fixed as suggested above. The same procedure has been used to fix the CAS/CBS curve. The results are shown in Fig. 4, while the calculated vibrational term values are in Table 2. As in the cases of N_2 and O_2, the results are of high accuracy when compared with the empirical data. We observe that most vibrational levels that would be obtained in a more pragmatic way by ignoring outliers (the points that violate the form of a smooth potential curve) do not differ significantly from those here reported.

Some further remarks on the accuracy of the present scheme may be extracted from Fig. 5, which compares the results obtained from the present approach with those

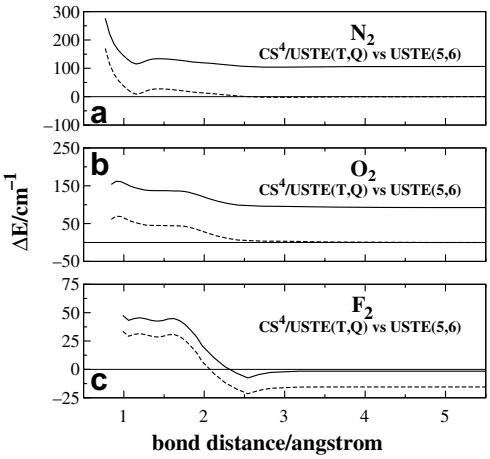

Fig. 5. Difference between the potentials obtained by extrapolating the dynamical correlation at the two highest affordable cardinal numbers, USTE(5,6), and the CS^4/USTE(3,4) ones: (a) N_2; (b) O_2; (c) F_2. The dashed lines are the deviations in relative energy (with respect to the asymptote), and the solid lines in absolute energy.

obtained by utilizing dynamical correlation energies scaled pointwise from MRCI(Q) calculations with the two large affordable basis sets, namely using USTE(5,6). First, we observe that except for short distances in the repulsive wing of the potential curve, the absolute error seldom reaches an unsigned value larger than 125 cm^{-1} for both N_2 and O_2, and 40 cm^{-1} for F_2. When looking at relative energies, such values reduce in the above order to 50 and 25 cm^{-1}.

Table 4 gathers the calculated equilibrium geometries as obtained from a parabolic fit to the three points with

Table 4
Deviations of raw and extrapolated equilibrium geometries[a] and dissociation energies[b] of N_2, O_2, and F_2 with respect to the experimental values[c,d]

System/time	AV*DZ*[e]		AV*TZ*[e]		AV*QZ*[e]		CS[1e]		CS[2e]		CS[3e]		CS[4e]		exp.[f]	
	ΔR_e	ΔD_e	ΔR_e	ΔD_e	ΔR_e	ΔD_e	ΔR_e	ΔD_e	ΔR_e	ΔD_e	ΔR_e	ΔD_e	ΔR_e	ΔD_e	R_e	D_e
N_2	0.026	42.28	0.011	16.72	0.008	7.57	0.006	2.01	0.006	2.17	0.006	2.17	0.006	2.17	1.09768	−364.046
							0.006	1.66	0.006	1.71	0.006	1.71	0.006	1.71		
CPU time[g]	0.30		0.60		1.99											
O_2	0.020	20.29	0.013	8.22	0.009	3.48	0.007	0.74	0.007	0.69	0.007	0.69	0.007	0.68	1.20752	−191.540
							0.006	0.52	0.006	0.46	0.006	0.46	0.006	0.46		
CPU time[g]	0.22		0.44		1.59											
F_2	0.041	14.15	0.014	5.38	0.009	3.85	0.006	2.76	0.006	2.67	0.006	2.67	0.006	2.67	1.41193	−62.663
							0.006	2.79	0.006	2.69	0.006	2.69	0.006	2.69		
CPU time[g]	0.03		0.17		1.13											

Also indicated are the CPU times for a MRCI/AV*XZ* calculation at the equilibrium geometry (pivot #1).
[a] $\Delta R_e = R_e^{calc} - R_e^{exp}$, where the superscripts 'calc' and 'exp' stand in an obvious correspondence for calculated and experimental.
[b] $\Delta D_e = D_e^{calc} - D_e^{exp}$.
[c] Bond distances are in angstrom, energies in millihartree, and times in minutes.
[d] The corresponding deviations $(\Delta R_e, \Delta D_e)$ for the MRCI(Q)/AV5Z and MRCI(Q)/AV6Z calculations are (0.007,4.79) and (0.007,3.66) for N_2, (0.008, 2.23) and (0.007, 1.64) for O_2, and (0.007, 3.39) and (0.007, 3.17) for F_2.
[e] Notation of theoretical methods as in previous Tables.
[f] Refs. [20,28].
[g] The CPU times, in minutes, are for a MRCI(Q) calculation. For MRCI(Q)/AV5Z and MRCI(Q)/AV6Z calculations, they are: 8.95 and 39.90 for N_2; 7.79 and 36.31 for O_2; 6.45 and 31.5 for F_2. The CPU times for CAS/AV*DZ* to CAS/AV6Z calculations are: 0.01, 0.07, 0.55, 3.78 and 20.60 for N_2; 0.01, 0.07, 0.55, 3.81 and 20.80 for O_2; 0.01, 0.07, 0.57, 3.72 and 20.65 for F_2.

lowest energy. Note that by choosing pivot #1 to coincide with the experimental equilibrium geometry by no means implies that the latter will coincide with the minimum of the extrapolated curves. This is seen to exceed experiment by 0.006–0.007 Å while the well depths are 0.7–2.2 mE_h (0.4–1.4 kcal mol^{-1}) too shallow when compared with experiment [20]. Our results are found to compare well with explicitly correlated MR-CI estimates (often corrected for the basis set superposition error): e.g., Ref. [27] for N_2 which also gives references to earlier work. One should recall at this stage that we have ignored core-correlation effects by considering only 10 (2s and 2p) correlated electrons. Additionally, we could not account for the inescapable intrinsic error of the wave function model or the corrections due to relativistic effects and breakdown of the Born-Oppenheimer approximation. One hopes, that consideration of such effects will enhance the predictive capabilities of our scheme.

A final issue concerns the cost of the present approach when used to calculate a PES. Its efficiency with respect to a scheme based on the pointwise extrapolation from MRCI(Q)/AV5Z and MRCI(Q)/AV6Z energies can be assessed by the ratio

$$\eta = \frac{N_p\left(\tau_6^{\mathrm{MRCI}(Q)} + \tau_5^{\mathrm{MRCI}(Q)}\right)}{N_p\left(\tau_D^{\mathrm{MRCI}(Q)} + \tau_T^{\mathrm{MRCI}(Q)} + \tau_5^{\mathrm{CAS}} + \tau_6^{\mathrm{CAS}}\right) + N\tau_Q^{\mathrm{MRCI}(Q)} + (N_p - N)\tau_Q^{\mathrm{CAS}}} \quad (14)$$

where N_p and N have the meaning assigned in Section 1, and τ_X are the timings of the various calculations (indicated as superscript). Typical CPU times obtained from a single calculation at the geometry of pivot #7 are gathered in Table 4. Because the CAS/AV5Z and CAS/AV6Z calculations (including the ROHF cycle [19]) are rather expensive, the above ratio is $\eta \sim 2$. An obvious way to further enhance the efficiency of our method is by using an extrapolation scheme for the CAS energy that employs raw energies with cardinal numbers no larger than $X = Q$. For this, we have tested the two-parameter formula of Karton and Martin [13]. Although still yielding reasonable values, a generalization of our extrapolation rule [10] that uses such data seems to underestimate the best CAS/CBS energies, while a fit using Eq. (4) usually leads to an overestimation. As Table 4 shows, the (R_e, D_e) attributes of the potentials so obtained are typically within the accuracy of a MRCI(Q)/AV7Z calculation or so when judged from the experimental data, although some differences occur in the spectroscopy of O_2 for which we could not find a simple explanation. The η ratios vary now from 29 for N_2 with 4 pivots to over 48 for F_2 with 1 pivot. Note that the CPU time savings are still large when comparing a CS^1/USTE(T, Q) potential based on a (T, Q) extrapolation of the CAS energy with a raw MRCI(Q)/AV5Z calculation. The ratios are in this case of $\eta = 6.0$, 6.3, and 6.2 for N_2, O_2, and F_2, respectively. In summary, the CS^N/USTE(T, Q) potentials here reported can achieve a performance only matched by MRCI(Q)/AV6Z or even higher quality potentials, but at a much lower computational cost. This, added to the fact that AV*QZ* basis sets are often just affordable for many systems of interest, makes the present scheme also promising in such cases.

4. Conclusions

We have generalized our previously reported scheme [15] that enables a potential energy surface corresponding

to a calculation with a large basis set to be obtained from small basis sets calculations. The idea of scaling the correlation energy at a single pivot has accordingly been extended to include an arbitrary number of pivots. The application of the method to achieve the one-electron basis set limit has also been explored. Although the multi-pivot schemes have shown to yield curves that mimic the raw *ab initio* curve calculated at the target basis set level better than CS[1] by factors of fivefold or more, this by no means implies that the potentials so generated lead to a better agreement with the available spectroscopic data. This has partly been ascribed to the theoretical method utilized to calculate the raw data, namely the MRCI(Q) method which is known to suffer from size-extensivity errors. Irrespective of the number of pivotal geometries used for correlation scaling, the new methods suggest that highly accurate potentials can be obtained with modest basis sets that are often considered obsolete for quantitative purposes. This may lead to savings in computer time up to a factor of about 50 smaller than when attempting the direct solution of the non-relativistic electronic Schrödinger equation using MRCI(Q)/AVXZ methods. Although the method has been tested on diatomic curves, there is no reason of principle why it should not work for polyatomic molecules. For example, in the case of an A–BC interaction, the common strategy is to scan cuts for fixed values of the Jacobi angle, which very much resemble diatomic potentials. Of course, maxima may occur along such cuts as indeed it also happens in some diatomic systems, e.g., the $A^1\Pi$ state of CO. Work under way for this system indicates though that the method can yield equally successful results. Finally, the method may offer a promising route for accurate dynamics on-the-fly.

Acknowledgements

This work has been supported by Fundação para a Ciência e Tecnologia, Portugal (contracts POCI/QUI/60501/2004, POCI/AMB/60261/2004, and REEQ/128/QUI/2005).

References

[1] T. Helgaker, P. Jørgensen, J. Olsen, Molecular Electronic-Structure Theory, Wiley, Chichester, 2000.
[2] H.-J. Werner, P.J. Knowles, J. Chem. Phys. 89 (1988) 5803.
[3] P.J. Knowles, H.-J. Werner, Chem. Phys. Lett. 145 (1988) 514.
[4] T.H. Dunning Jr., K.A. Petersson, D.E. Woon, in: P.v.R. Scleyer, N.L. Allinger, T. Clark, J. Gesteiger, P.A. Kolman, H.F. Schaefer III (Eds.), Encyclopedia of Computational Chemistry, Wiley, Chichester, 1998, p. 88.
[5] Basis sets were obtained from the Extensible Computational Chemistry Environment Basis Set Database, Version 02/25/04, as developed and distributed by the Molecular Science Computing Facility, Environmental and Molecular Sciences Laboratory which is part of the Pacific Northwest Laboratory, P.O. Box 999, Richland, Washington 99352, USA, and funded by the U.S. Department of Energy. The Pacific Northwest Laboratory is a multi-program laboratory operated by Battelle Memorial Institute for the U.S. Department of Energy under contract DE-AC06-76RLO 1830. Contact Karen Schuchardt for further information.
[6] T. Helgaker, W. Klopper, H. Koch, J. Noga, J. Chem. Phys. 106 (1997) 9639.
[7] D.G. Truhlar, Chem. Phys. Lett. 294 (1998) 45.
[8] A.J.C. Varandas, J. Chem. Phys. 113 (2000) 8880.
[9] W. Klopper, Mol. Phys. 6 (2001) 481.
[10] A.J.C. Varandas, J. Chem. Phys. 126 (2007) 244105.
[11] C. Schwartz, Phys. Rev. 126 (1962) 1015.
[12] W. Kutzelnigg, J.D. Morgan III, J. Chem. Phys. 96 (1992) 4484.
[13] A. Karton, J.M.L. Martin, Theor. Chim. Acta 115 (2006) 330.
[14] A.J.C. Varandas, Phys. Scr. (Comm. At. Opt. Mol. Phys.), in press.
[15] A.J.C. Varandas, P. Piecuch, Chem. Phys. Lett. 430 (2006) 448.
[16] F.B. Brown, D.G. Truhlar, Chem. Phys. Lett. 117 (1985) 307.
[17] A.J.C. Varandas, J. Chem. Phys. 90 (1989) 4379.
[18] P.L. Fast, J. Corchado, M.L. Sanchez, D.G. Truhlar, J. Phys. Chem. A 103 (1999) 3139.
[19] H.-J. Werner, et al., MOLPRO, version 2002.6, a package of ab initio programs, see www.molpro.net, 2003.
[20] K.P. Huber, G. Herzberg, Molecular Spectra and Molecular Structure IV. Constants of Diatomic Molecules, Van Nostrand, New York, 1979.
[21] S. Edwards, J. Roncin, F. Launay, F. Rostas, J. Mol. Spectrosc. 162 (1993) 257.
[22] R.J. LeRoy, LEVEL 7.5, A computer program for Solving the Radial Schrödinger Equation for Bound and Quasi-bound Levels, University of Waterloo Chemical Physics Research Report CP-655, 2002.
[23] W. Duch, G.H. Diercksen, J. Chem. Phys. 101 (1994) 3018.
[24] P.H. Krupenie, J. Phys. Chem. Ref. Data 1 (1972) 423.
[25] A.J.C. Varandas, S.P.J. Rodrigues, V.M.O. Batista, Chem. Phys. Lett. 424 (2006) 425.
[26] A.S. Cheung, K. Yoshino, J.R. Esmond, W.H. Parkinson, J. Mol. Spectrosc. 178 (1996) 66.
[27] R.J. Gdanitz, Chem. Phys. Lett. 283 (1998) 253.
[28] E.A. Colbourn, M. Dagenais, A.E. Douglas, J.W. Raymonda, Can. J. Phys. 54 (1976) 1343.
[29] C. Ciping, D.A. Ramsey, J. Mol. Spectrosc. 160 (1993) 512.
[30] G. Rouillé, G. Millot, R. Saint-Loup, H. Berger, J. Mol. Spectrosc. 154 (1992) 372.
[31] R.A. Copeland, P.C. Cosby, D.R. Crosley, J.B. Jeffries, T.G. Slanger, J. Chem. Phys. 86 (1987) 2500.
[32] V.N. Snopko, Opt. Spectrosc. 29 (1970) 445.
[33] M. Ogawa, Sci. Light 15 (1966) 97.
[34] H.D. Bacock, G. Herzberg, Astrophys. J. 108 (1948) 167.
[35] W. Lochte-Holtgreven, G.H. Dieke, Ann. Phys. 3 (1929) 937.